Advances in Environmental Technology 12(3) 2026, 375-395.

Iranian Reasearch Organization for Science and Technology (IROST)

Advances in Environmental Technology

Journal home page: https://aet.irost.ir

Optimization studies of chromium biosorption by carbon nanoparticles of *Cocos nucifera*

Adimoolam Saravana Raj[a]*, Aakaash Karuppaiah Subramanian[a], Vinosh Muthukumar Perumal[a], Bharathiraja Balasubramanian[b], Veeramalini Jayabalan[a], Saravana Kumar Ganesan[c,d], Meenakshi Sundar Akilan[e]

[a] *Department of Chemical Engineering, Vel Tech High Tech Dr. Rangarajan Dr. Sakunthala Engineering College, Avadi, Chennai, Tamil Nadu, India.*

[b] *Department of Biotechnology, Easwari Engineering College, Ramapuram, Tamil Nadu, Chennai, India.*

[c] *Department of Computer Science and Engineering, Karpagam Academy of Higher Education, Coimbatore-641021, India.*

[d] *Centre for Artificial Intelligence and Autonomous Aerial Systems (CAAAS), Karpagam Academy of Higher Education (Deemed University), Coimbatore-641021, India.*

[e] *Department of Chemical Engineering, V.S.B. Engineering College, Karur, Tamil Nadu, India.*

ARTICLE INFO

Document Type:
Research Paper

Article history:
Received 27 August 2024
Received in revised form
20 June 2026
Accepted 21 June 2026

Keywords:
Carbon nanoparticles
Cocos nucifera
Leather effluent treatment
Response surface optimization
Langmuir isotherm

ABSTRACT

Carbon nanoparticles (CNPs) were produced from the leaves of *Cocos nucifera* and chemically activated using phosphoric acid. The activated CNPs were characterized using Brunauer-Emmett-Teller (BET) (surface area: 122.53 m^2/g; mean pore diameter: 16.29 nm) and Field Emission Scanning Electron Microscopy (FE-SEM) (particle size: 20-30 nm). Batch adsorption experiments were conducted to optimize chromium (VI) removal from leather industry effluent. Response surface methodology with Central Composite Design (CCD) was employed to investigate the effects of four parameters: Cr concentration (10-100 ppm), CNP dosage (1-10 g/L), contact time (10-60 min), and pH (1-7). Under optimized conditions (Cr concentration 100 ppm, CNP dosage 10 g/L, contact time 30 min, and pH 2), the maximum removal efficiency achieved was 83% with an adsorption capacity of 83 mg/g. ANOVA analysis confirmed the quadratic model adequacy (F-value = 74.65, $p < 0.0001$, and $R^2 = 0.9896$). CNP concentration emerged as the most influential parameter. Isotherm modeling analysis demonstrated that the chromium biosorption process follows Langmuir isotherm behavior with an R^2 value of 0.9951, a Chi-squared error (χ^2) value of 0.2452, and a root mean square error (RMSE) of 1.0002 mg/g, indicating monolayer adsorption. The *Cocos nucifera* carbon nanoparticles demonstrated high efficiency for chromium removal from tannery effluents under acidic conditions.

*Corresponding author Tel.: +99 52653257
E-mail: saravanarajchemical@gmail.com
DOI: 10.22104/aet.2026.6958.1948

1. Introduction

The coconut palm (*Cocos nucifera*) is found throughout the tropics, where it is inextricably linked to the daily lives of locals. The coconut is thought to have originated in Indo-Malaya and spread throughout the world. For one amazing reason, it is being called the "tree of life" and "tree of heaven" [1]. Today, it is an important subsistence and economic crop in most small Pacific Island countries. It prefers warm, humid conditions but can tolerate temperatures as low as 21 °C for brief periods of time [2]. Low-lying islands in the Pacific are extremely dependent on it because it gives them access to nearly all of the necessities of life in the absence of land-based natural resources, including food, drink, fibre, medicine, oil, timber, mats, fuel, and household utensils [3]. It is simple to recognize, thanks to the clusters of large fruits carried atop long, slender stems and the crown of feather-like fronds on which it grows.

Approximately 90% of tanning industries use alkaline chromium sulphate as a tanning agent in leather tanning [4], with the pickle pelt absorbing 60% and the remaining 40% in the spent chrome liquor [5]. In general, a large amount of foreign exchange is earned by tannery industries through the export of leather goods [6]. The emission of untreated tannery effluents often contains high amounts of Mg, Ca, NaCl, sulphides, trivalent, and hexavalent chromium (HC). BOD and COD impact ecosystem flora and fauna as well as human health. So far, no process has been identified for removing all types of waste found in wastewater from tannery industries [7]. Chemical reduction and oxidation, liquid extraction, membrane separation, carbon adsorption, electrolytic treatment, ion exchange, coagulation, electro-precipitation, flotation, evaporation, crystallization, ultrafiltration, and electrodialysis have all been used to remove HC from aqueous bodies.

Heavy metal contamination of surface water and wastewater is a serious issue for both the environment and public health [8]. Metal plating plants, tanneries, mining, and other industries that produce heavy metal pollution pollute marine and freshwater environments [9]. When heavy metal concentrations in wastewater exceed safe levels, they can endanger livestock, the aquatic environment, and human health [10]. Skin rashes and other serious diseases are caused by trivalent chromium, whereas HC is far more dangerous and can result in serious health consequences such as lung cancer and headache [11]. Chromium and several other heavy metals present in the effluents of the brassware industry in Morocco were causing human health and biodiversity risks, as reported in an article; it was also reported that biological treatments were insufficient to completely treat the effluents before releasing them into farmland [12].

There are over 2,000 tanneries in India. The wastewater generated during the tanning chroming phase contains 1500–3000 mg/L of chromium, while the wastewater generated by the tannery sector at the conclusion of all operations contains 80–200 mg/l. Environment Protection Rules, 1986 (Schedule VI), state that the acceptable limit for Cr is 2 mg/L in wastewater from industries. According to IS 10500:2012, the acceptable limit for potable water is 0.05 mg/L [13]. In excess, it can cause short and long-term harmful effects: shortness of breath, wheezing, coughing, abdominal discomfort, vomiting, and hemorrhage, as well as neurological effects [14,15]. Also, aquatic systems are prone to being affected seriously due to heavy metal pollution since they are the end recipients in most cases [16]. HC can also cause cancer [17].

Environmental standards are being established in order to effectively regulate the quantity of heavy metals released into water sources, and industrial output is now being rigorously supervised. Chromium is a common ingredient in leather tanneries, electroplating, chromate preparation, and metal finishing [18].

In the environment, chromium is a redox active metal element that is typically found as Cr(III) or Cr(VI). Chromate (CrO_4^{2-}), dichromate ($Cr_2O_7^{2-}$), and hydrochromate ($HCrO_4^-$) are the three forms that HC can prevail. On the other hand, Cr(III) in aqueous solutions might exist as $Cr(OH)^{2+}$, $Cr(OH)_2^+$, and Cr^{3+}. Compared to Cr(III), hexavalent chromium is more harmful to living things [19].

In industrial processes, the adsorption method of treating effluents is a viable and widely utilized

approach [20]. The use of adsorbents made from free, natural sources has piqued the interest of researchers worldwide due to their numerous advantages, including reusability and cost-effectiveness. Chemical adsorption, as opposed to physical adsorption, requires a separate activation energy for atom transfer to the adsorption surface [21]. The adsorption technique using activated carbons is popular due to its effectiveness, low operational cost, and high adsorption capacity; it is considered appropriate among other conventional methods [22]. Lower-cost, readily available adsorbent materials for heavy metal ion removal from sewage water are currently being developed from agricultural and various solid biomass waste substances. Adsorption of organic compounds by CNPs in aqueous phases is a promising and well-proven water treatment methodology for environmental protection [23].

Among the various agricultural waste materials explored for heavy metal biosorption, *Cocos nucifera* leaves were selected as the carbon precursor material in this study for several strategic reasons. First, coconut is one of the most abundantly cultivated tropical crops, with India alone producing millions of tonnes of coconut annually, making coconut leaves a readily available and cost-effective biomass resource. Second, coconut leaf biomass is typically discarded as agricultural waste; thus, utilization for CNP production represents an environmentally sustainable approach to waste valorization. Third, preliminary experimental trials demonstrated that coconut leaves possessed higher carbon content and a porous structure suitable for chemical activation compared to other coconut components. Fourth, the abundant presence of cellulose and lignin in coconut leaves provides excellent precursor material for producing carbon nanoparticles with well-developed pore structures through appropriate carbonization and chemical activation with phosphoric acid. Finally, literature reports indicate that CNPs derived from coconut waste materials have demonstrated promising adsorption capacities for heavy metals, including chromium, lead, and copper. The combination of ready availability, sustainability, economic viability, and proven adsorption potential made *Cocos nucifera* leaves the optimal choice for this investigation [21-24]. Despite the extensive literature on chromium adsorption using various adsorbent materials, the potential application of *Cocos nucifera* leaf-derived carbon nanoparticles for chromium removal from leather industry effluents remains unexplored. The primary objective of this study is to develop and optimize a biosorption process utilizing *Cocos nucifera* carbon nanoparticles for removing hexavalent chromium from leather tannery effluent

2. Materials and methods

2.1. Preparation of CNP

Cocos nucifera leaf particles of 200 to 250 m in size were soaked in phosphoric acid solution after being shredded, crushed, powdered, and oven-dried at 90 °C for 24 hours. 10 grams of *Cocos nucifera* leaf powder, precisely weighed, was dispersed in 100 milliliters of phosphoric acid solution and stirred for a day at 90 °C. The solution was then left at room temperature for twenty-four hours before being stirred once every four hours. In a hot air oven, the saturated leaf powders were dried at 115 °C for a day before being placed in an electrical furnace with a nitrogen flow rate of 100 mL/min and a heating rate of 10 °C per minute until 700 °C for one hour. The material was then soaked for one day in a 1 N hydrochloric acid solution, cleaned, and dried in a hot air oven at 115 °C for one day before being stored for experiments and analysis.

2.2. Adsorbate

The accurately weighed 2.8287g of 99.9% $K_2Cr_2O_7$ (Cr=51.99, $K_2Cr_2O_7$=294.125) was dissolved in 1000mL of water. This mixture was diluted to produce a typical solution containing 30-300 mg/L of HC. By adding 0.5 N HCl/NaOH, the solution's pH level was adjusted.

2.3. Batch adsorption studies

Batch adsorption experiments were conducted with known quantities of adsorbents (CNP) and an effluent solution containing varying concentrations of HC at various pH values. In a temperature-controlled rotary shaker, the reaction mixture was agitated at a constant rpm. Based on the experimental design, adsorbate concentration, and adsorbent concentration, the reaction time

and pH of each reaction were fixed. To find the optimum process condition for maximum efficiency, 26 experimental trials were conducted in triplicate. The system's temperature was kept constant at 30±2°C. Leather tannery effluent typically exits treatment operations at ambient to moderately warm temperatures (25-35°C) under normal operational conditions. Maintaining experiments at 30±2°C simulates realistic industrial wastewater treatment scenarios, enabling direct application of results to full-scale treatment systems.

Using an AA-203 Atomic Adsorption Spectrophotometer, the quantity of HC retained by CNP was found. The following expression was used to compute the Cr (VI) percentage adsorbed from the solution.

$$R = [(C_i - C_e)/C_i]x100 \quad (1)$$

where C_e represents the final concentration and C_i represents the initial concentration.

The mass balance on the adsorbed species in a system was used to determine the adsorption capability of CNP. The succeeding equation is used to calculate C. *nucifera's* adsorption capacity for each HC concentration:

$$q_e = [(C_i - C_e)/M]xV \quad (2)$$

where q_e is the adsorption capacity in mg/g, M is the mass of adsorbent in grams, and V is the volume of solution in liters.

2.4. Design of Experiments (DoE)

An analysis of cause-and-effect relationships through DoE is a methodical process. Statistically, the experiment on the adsorption of chromium hexavalent over CNP was designed to find common relationships between various factors that influence the process to find the best conditions. For a research design methodology to be cost-effective, it must be able to extract as much complex information as possible while reducing experimental time and saving money on both material and personnel costs. Experiment design using central composite design (CCD) and response surface methodologies (RSM) are common. ANOVA is not a test, but rather a technique that follows the principle of breaking down a complete dataset into smaller groups based on sources of variation. This serves to test the consistency of the suggested hypotheses for model parameters [24].

In our study, a Central Composite Design RSM module was employed to enhance the efficacy of reducing the concentration of chromium from leather industrial effluents. To analyze the removal efficiency, four process variables, including chromium concentration (A), CNP concentration (B), Time (C), and pH (D), were considered for optimization. The F-value decreases in magnitude as the corresponding coefficient increases in significance. In addition to this, the F-test was utilized to determine the R^2 coefficient in the regression equations. Model sufficiency can also be assessed using the Lack of Fit (LoF) diagnostic test, which compares pure error derived from replicate measurements to LoF based on model performance.

3. Results and discussion

3.1. Cr (VI) adsorption onto the CNPs

The utilization of carbon nanoparticles derived from different natural sources was employed in the process of bioremediating heavy metal contamination. Based on an extensive literature survey and preliminary experimental studies, five important parameters influencing the bioremediation of chromium effluent were considered and their effects are discussed in our present study. The optimized process parameters are shown in Table 1 below.

Table 1. Optimum process parameters for chromium biosorption on *Cocos nucifera* carbon nanoparticles.

Parameter	Optimum Value	Range Investigated
Chromium (VI) Concentration	100 ppm	10 to 100 ppm
CNP Dosage	10 g/L	1 to 10 g/L
Contact Time	30 min	10 to 60 min
pH	2.0	1 to 7

When all four parameters are operated simultaneously at their optimum values, the integrated synergistic effects result in the maximum overall removal efficiency of 83%, with an adsorption capacity of 83 mg/g. This indicates that no single parameter dominates the process, and balanced optimization of all variables is critical for achieving maximum performance. The process

parameters considered for optimization by various other researchers are shown in Table 2.

3.1.1. Effect of agitation speed

In this adsorption procedure, the agitation speed was observed to be significant. The agitation speed was fixed based on the initial experimental trials and through an extensive literature survey. A constant value of 150 rpm was maintained for all our experiments conducted. Based on previous research, it was found that increasing the speed of agitation led to improved movement of chromium hexavalent ions towards the adsorbent surface. This was brought on by a narrowing of the boundary layer that surrounded the adsorbent particles. Also, at 150 rpm, the percentage of lead adsorbed reportedly reached the maximum (95%) compared with lower or higher rpm values [25]. It was reported that the best agitation speed for all the experiments was maintained at 150 rpm [26].

3.1.2. Effect of pH

The pH ascertains the adsorbate's speciation, adsorbents' surface charge, and ionization degree. Also, the adsorbate-adsorbent electrostatic interaction depends on the pH value of the solution [27]. The graph in Figure 1 shows that when the pH value of the solution increases, the ability to eliminate HC from pollutants is significantly reduced. When the preliminary chromium concentration was considered at an ideal pH level of 2, the removal percentage efficiency of 83% was observed. CNP dosage and contact time were 100 ppm, 10 g/L, and 30 min, respectively.

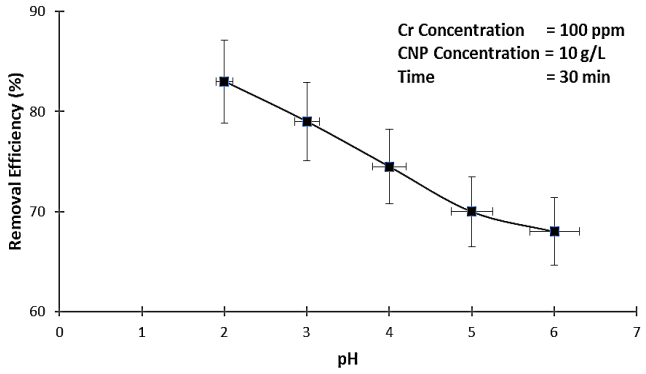

Fig. 1. Percentage removal of chromium at different pH.

Similar studies by various researchers reported that at a pH of 1.5, the HC adsorption was found to be at maximum (83 %); later, when the pH was varied between pH 1.5 and 7, the adsorption efficiency decreased to 36 %. The surface that absorbed the anionic hydroxy group (-OH) has an attraction to H+ ions at low pH levels, and as a result, the efficiency suffers. To test the impact of different pH levels on Cr6+ adsorption, researchers conducted experiments and observed an increase in efficiency from 75% to 86% when the pH was raised from 2 to 6. Between pH values ranging from 6.5 to 9, the efficiency gradually declined from 85 to 33 percent [21]. Most literature studies focused on examining the impact of pH values in terms of adsorption of HC between the pH range of 2.0 and 7.0. It was found that the solution's pH level had a big impact on getting rid of HC, with the most significant removal (85%) occurring at a pH of 2.0. It was observed from literature that the pH level significantly influences the adsorption of HC, as the adsorption capacity was found to decrease when the pH was varied from 2.0 to 7.0 [26].

Another study explored the impact of lead adsorption rate with varying pH levels from 3 to 7, with a maximum limit of 7 to prevent lead precipitation. It was concluded from the study that the pH level of aqueous environments is a vital indicator of the configuration of metallic substances, as it affects the charge of metal ions, which in turn influences adsorption. It was also observed that lead (II) species with a positive charge are dominant at low pH levels, despite the fact that different lead species have different charges at elevated pH levels ranging from 7 to 11 [25]. In a similar study, at a constant adsorbent dose of 14 g/L, three different biosorbents at three different reaction times were tested to improve the percentage of chromium reduction at pH 10. The adsorption efficiency was found to be 95.42%, 88.38%, and 83.57% for the three sorbents. It was concluded that the increase in pH enhances the % of chromium removal due to the attaching site deprotonation [18]. Similarly, an adsorbent prepared from spent coffee grounds, when used to remove Cr (VI), yielded similar results; the adsorption was found to decrease as the pH rises. A 91% removal rate was achieved under optimal extraction conditions, such as pH 2, an adsorbent dose of 0.2 g in 100 mL at 120 min equilibration time, 300 rpm, and 303 K [28]. Biochar particles from

Onopordom heteracanthom, when treated with wastewater, show that when the pH level increases, the rate of adsorption for HC decreases. When the pH level was at 1, 2, 3, and 4, the percentage of HC adsorption onto BCP was 88%, 69%, 6%, and 0.5%, respectively [29]. When *Acacia albida* and *Euclea schimperi* were used as adsorbents, they had a similar effect. At pH 2, *Acacia albida* uptake percentage value was 98.47%, and that of *Euclea schimperi* was 97.39%. It is clear from this observation that adsorption efficiency is very high at low pH [30].

3.1.3. Effect of adsorbent dose

From 1 to 10 g/L, when the CNP dosage was gradually increased (Figure 2), there was a steady and proportional improvement in the removal efficiency of HC from the effluent. When the initial concentration of Cr, pH, and contact time were kept constant at 100 ppm, pH 2, and 30 min, respectively, 83% removal efficiency was the highest recorded.

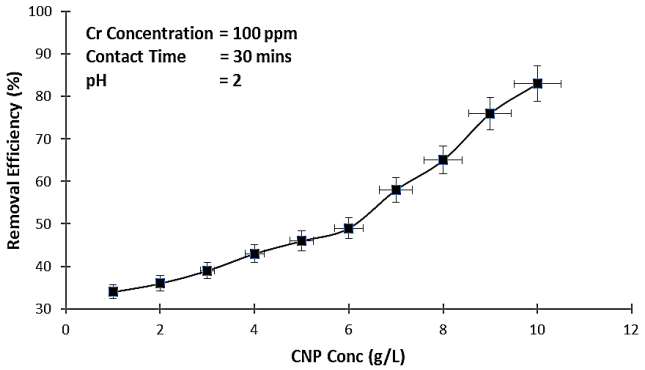

Fig. 2. Percentage removal of chromium at various CNP concentrations.

At an adsorbent concentration of 15 g/L, chromium's removal effectiveness was calculated to be 88.28%. In a study, it was discovered that the removal efficiency rose from 53.3% to 84.1% as the amount of adsorbent was raised from 1.5 to 10 g/L. This suggests that the adsorbent dosage has a significant impact on the removal efficiency, increased dosage results in increased Cr 6+ removal efficiency. While maintaining the same values for other factors like contact time and pH, the adsorbent dosage increased from 1.5 to 25.5 g/L. The Cr removal efficiency increased gradually and remained constant after reaching a maximum value of 20 mg/L [21]. The effect of activated carbon as an adsorbent for HC was studied, and it was concluded that the time required to reach equilibrium decreased with increasing adsorbent dose. A range of adsorbent dosages from 0.01 to 0.07 g/100 mL of HC solution was investigated for three hours. Maximum adsorption capacity was observed with 0.05g, and there was not much variation in the adsorption beyond 0.05g [26]. Maximum adsorption capacities of 91.79, 78.60, and 85.71 percentage was achieved for the three different adsorbents S1, S2, and S3, respectively, and it was reported that the rapid removal of metals was due to the increased accessibility of exchangeable sites or surface area of the adsorbents [18]. The use of pomegranate seed as a sorbent also yielded successful results. When a dosage of 0.6 g per 100 mL was applied, the maximum removal percentage for HC ions was found to be 99.5% and 96.2% for concentrations of 2 and 10 mg per L, respectively [31].

3.1.4. Effect of initial HC concentrations

Based on the graph presented in Figure 3, it is noted that as the effluent's initial chromium concentration rises, the removal capacity of hexavalent also increased significantly. The highest removal capacity was found to be 83 mg per g at an initial chromium concentration of 100 ppm when the adsorbent dosage was 10 g per L, the contact time was about 30 min, and the pH was 2.

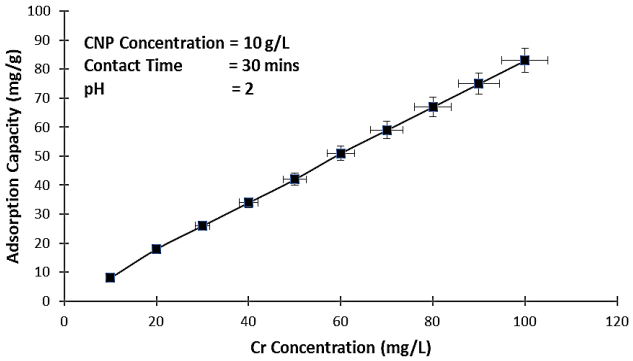

Fig. 3. Adsorption capacity against initial chromium concentration.

In a prior study with similar conditions, the concentration range observed was 5 gm/L to 100 gm/L. The highest efficiency of 87.3% was found at a concentration of 50 mg/L. Increasing the concentration of chromium resulted in a higher removal efficiency. Conversely, reducing the

concentration caused the maximum adsorption efficiency to gradually decline [21].

In accordance with the report, the HC adsorption capacity initially increased rapidly, but then slowed down until a state of equilibrium was achieved, indicating that the adsorption process reached its maximum potential.

In all concentrations tested, the absorbent was found to remove significant amounts of HC during the initial 20 min of contact time, and balance was achieved after 60 min.

This is likely due to the abundance of available active functional groups and, early on in the adsorption process, there are empty sites on the adsorbent surface. In a separate study, it was seen that increasing the initial concentration of chromium hexavalent from 10 mg per L to 25 mg per L led to an increase in the equilibrium adsorption from 19.18 mg per g to 43.45 mg per g. However, the percentage removal of chromium hexavalent decreased from 99.08 to 86.89 percent [26].

The research aimed to eliminate chromium hexavalent through the utilization of divinyl benzene copolymer resin. The findings indicated that the proportion of removal was reduced from 99.8% to 80% when the amount of HC in the starting solution increased from 100 to 500 mg per L [32]. Thus, an initial concentration over and above an optimum level may affect the efficiency of the process.

3.1.5. Effect of contact time

The reasonable elimination rate of HC (77%) was found with a contact time of 15 min optimal time, an initial Cr concentration of 100 ppm, 10 g/L of adsorbent, and at a pH value of 2. As indicated by the graph in Figure 4, contact time has a direct relationship with removal efficiency.

A number of researchers have also identified particle size as being one of the critical factors for the successful removal of HC. In a particular study, the size of the particles used was between 75µm and 600µm, with an initial adsorbent concentration of 50 gm/L.

The study demonstrated that the highest removal efficiency was achieved with 75µm particles at a contact time of 10 hours, beyond which there was no significant increase in efficiency [21].

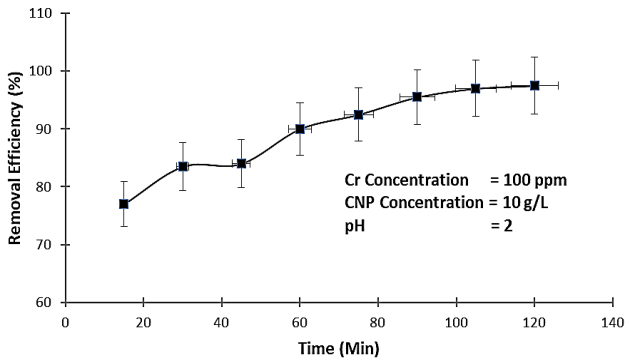

Fig. 4. Percentage removal of chromium against contact time.

Researchers have analyzed how contact time affects the removal of lead ions using both alumina-coated and uncoated carbon. Both adsorbents showed rapid lead uptake initially, followed by a gradual reduction in the adsorption rate after the first hour as equilibrium was approached. These results indicate that a contact time of 60 min is adequate to attain adsorption equilibrium. Additionally, the coated nanoparticles demonstrated a greater capacity for adsorption compared to the uncoated nanoparticles [25]. The duration of contact needed to achieve equilibrium is believed to be influenced by the starting concentrations of the components in the mixture, and the removal percentage progressively rises over time until samples with identical concentrations reach a state of equilibrium [18]. A previous study reported that activated carbon derived from Leucaena leucocephala is an effective adsorbent for the removal of hexavalent chromium through adsorption. The adsorptive removal of Cr (VI) showed a considerable increase within 30 min. Adsorption appeared to have reached equilibrium as the adsorption of Cr (VI) remained stable after 30 min [33].

3.1.6. Adsorption Isotherm

To understand the fundamental nature of the chromium biosorption process and its mechanistic characteristics, the experimental adsorption data were analyzed using standard isotherm models. The relationship between the amount of solute adsorbed (qe, mg/g) and the equilibrium concentration of adsorbate (Ce, mg/L) was investigated using two widely applied isotherm models. One is the Langmuir isotherm model [$q_e = (q_m \cdot K_L \cdot Ce)/(1 + K_L \cdot Ce)$], where q_m is the maximum

monolayer adsorption capacity (mg/g), and K_L is the Langmuir constant (L/mg); the other is the Freundlich isotherm model [$q_e = K_F \cdot Ce^{\wedge}(1/n)$], where K_F is the Freundlich constant (mg/g), and n is the adsorption intensity parameter. Preliminary data analysis, based on adsorption capacity data and equilibrium conditions achieved in all experimental runs, indicates that the chromium biosorption process onto carbon nanoparticles derived from *Cocos nucifera* follows the Langmuir isotherm behavior more closely than Freundlich behavior with an R^2 value of 0.9951 and a Chi-squared Error of 0.2452. This suggests the formation of a monolayer of chromium ions on the adsorbent surface, with saturation at approximately 83 mg/g and a Langmuir affinity constant (K_L) of 0.312 L/mg under optimal conditions, consistent with the Langmuir assumption. The Langmuir model fit (Figure 5) indicates relatively homogeneous distribution of adsorption sites on the carbon nanoparticle surface.

Unlike Freundlich behavior (Figure 6), which predicts multilayer adsorption on heterogeneous surfaces, the observed data suggest that once the monolayer is complete, additional chromium removal is minimal, as evidenced by the plateau in removal efficiency above CNP dosages of 10 g/L (Figure 2).

3.1.7. Field Emission Scanning Electron Microscopy (FE-SEM)

The CNP's surface morphology, which had a porous structure, was deemed appropriate for adsorption research. A Field Emission Scanning Electron Microscopy (FE-SEM) image (Figure 7) revealed that the carbon nanoparticles were within the size range of 20-30nm.

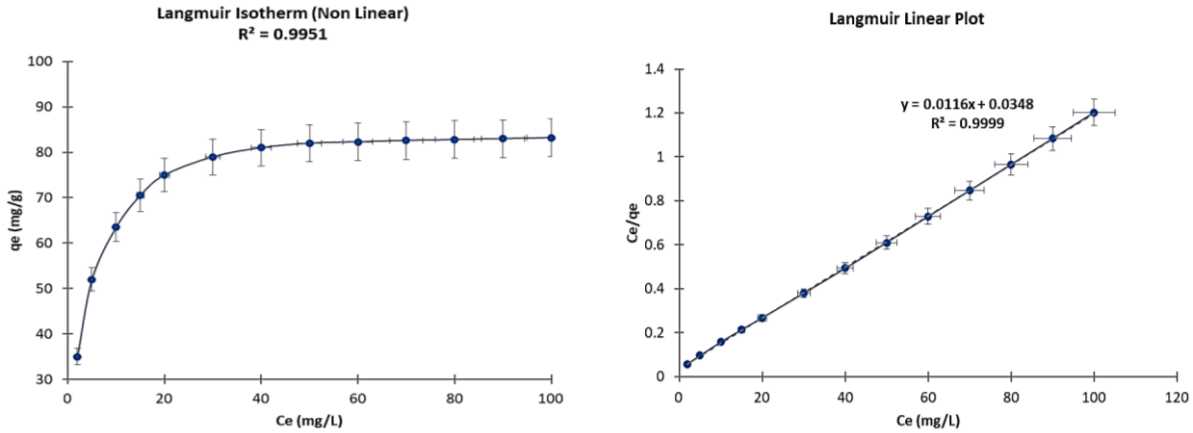

Fig. 5. Langmuir isotherm model fit of experimental adsorption data.

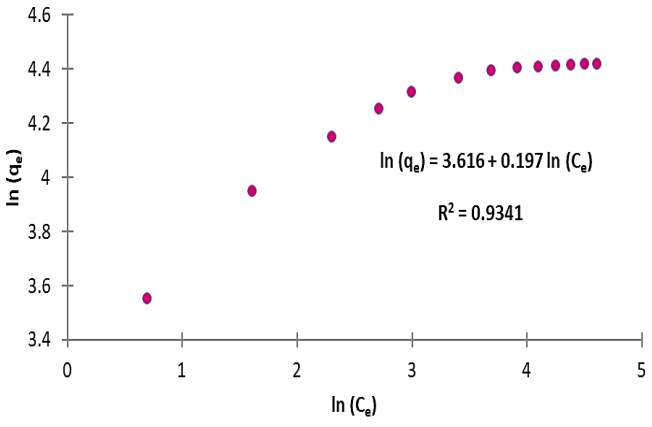

Fig. 6. Freundlich isotherm model fit of experimental adsorption data.

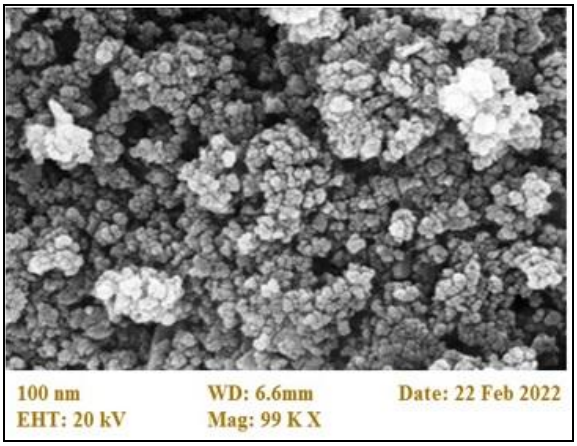

Fig. 7. FE-SEM of CNP.

Table 2. Optimized process conditions and adsorption capacity of carbon nanoparticles from various natural sources.

S. No.	Carbon Source	pH	Adsorbent dosage (g/L)	Contact Time (Min)	Chromium Concentration (ppm)	Adsorption efficiency (mg/g) or (%)	Ref.
1	Coconut shell	2	0.1	140	10	9.4	[34]
2	Ziziphus spina-christi leaf	2	5	55	10	97%	[35]
3	*Leucaenaleucocephala* seed pod	6	1	100	50	10	[36]
4	*Pisum sativum* peels	1.55	0.75	180	400	480	[37]
5	Corn Straw	3	0.1	540	50	175	[38]
6	*Juniperusprocera* leaves	4	0.1	120	70	96%	[39]
7	Castor seed	2	0.1	60	150	90%	[40]
8	Merck analytical grade	2	0.1	180	60	110	[41]
9	Bermuda Grass	2	0.5	1080	200	403	[42]
10	Lantana camara plant	2	4	30	150	26	[43]
11	Date Press Cake	2	1	180	300	283	[44]
12	Activated carbon from Chestnut oak shells	2	7	120	100	33	[45]
13	Camellia oleifera seed shell hydrochar	2	0.02	720	30	307	[46]
14	Alm8ond shell	2	2.5	240	1000	168	[47]
15	Ziziphus jujuba cores	2	1	360	100	196	[48]
16	Coffee Husk	2	3	60	100	5.7	[49]
17	Mango Kernel	2	2.5	150	80	7.8	[50]
18	African biomass waste (Peanut shells and Jatropha wood)	2	0.03	360	60	141	[51]
19	Walnut Shell-Based	3	1	300	100	59	[52]
20	Peanut shell and hybrid giant napier (Pennisetum hardum) straw	1.5	0.5	120	120	39	[53]
21	*Ricinus communis* Seed Shell	2	0.05	60	10	7.7	[54]
22	Tamarind wood	1	5	40	20	89%	[55]
23	Pomegranate husk	1	2	180	150	35	[56]
24	Date palm seed	1	4	180	75	120	[57]
25	Green alga *Ulva lactuca*	1	2	120	250	112	[58]
26	*Aegle Marmelos* fruit shell	2	3	180	10	43	[59]
27	Longan seed	3	0.5	360	100	35	[60]
28	Matured tea leaves	4.8	3	120	60	31	[61]
29	Tamarind seeds	2	10	3000	400	30	[62]
30	Rice straw	1	2	720	50	99%	[63]
31	Terminalia arjuna nuts	1	2	300	10	99%	[64]
32	*Hevea Brasilinesis* sawdust	2	0.01	300	200	44	[65]

3.1.8. Brunauer–Emmett–Teller (BET)

BET analysis is a dependable way to calculate the precise surface area of materials by measuring nitrogen multilayer adsorption as a function of relative pressure.

This technique measures both the external and internal (pore) surface areas of the sample, which is beneficial when investigating the effects of surface porosity and particle size for numerous applications. The mean pore diameter of CNP was found to be 16.29 nm using the BJH (Barrett, Joyner & Halenda) method of calculating pore size distributions. Additionally, the surface area of CNP was calculated from the BET analysis (Figure 8) to be 122.53 m^2/g.

3.2. ANOVA analysis

A mathematical equation (Eq. (3)) was developed to illustrate a comparison of the four independent variables considered for optimization by ANOVA. Additionally, the model equation was assessed using analysis of variance.

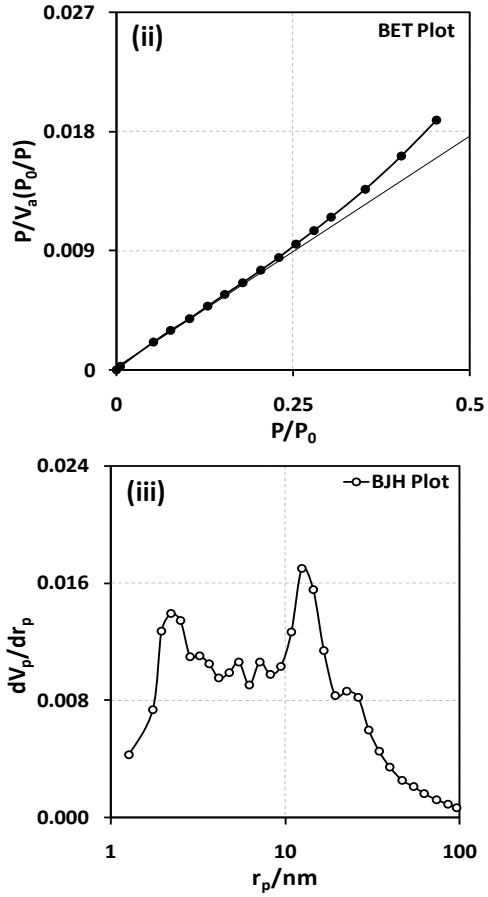

Fig. 8. BET of CNP.

The predicted model's coefficient terms and regression variables are presented in Table 3. The F and T values obtained from Tables 4 and 5 were used to determine the importance of each coefficient.

The model F value was calculated to be 74.65, with a T value of less than 0.0001, indicating that the model was noteworthy. The probability (P) value of B^2 was also lower than 0.0001, indicating that CNP concentration (B) was the most influential parameter among the four independent variables (A, B, C, and D) considered for optimization. The regression coefficient (R^2 = 0.9896) is evaluated from the quadratic model equation being closer to 1.0, indicating that the predicted values best suit the process of chromium biosorption by CNP.

$$\text{Removal efficiency} = +74.17 - 0.6667A + 25.58B + 1.21C - 5.04D + 0.8750AB - 0.5000AC - 1.50AD + 2.00BC - 4.25BD + 0.6250CD - 5.37A^2 - 12.75B^2 + 1.44C^2 - 3.19D^2 \quad (3)$$

Table 3. Coefficient Estimate and Standard Error values of interacting parameters.

Factor	Coefficient Estimate	Standard Error
Intercept	74.17	1.49
A-Cr Conc	-0.6667	0.8924
B-CNP Conc	25.58	0.8924
C-Time	1.21	0.8924
D-pH	-5.04	0.8924
AB	0.8750	0.9116
AC	-0.5000	0.9116
AD	-1.50	0.9116
BC	2.00	0.9116
BD	-4.25	0.9116
CD	0.6250	0.9116
A^2	-5.37	0.9802
B^2	-12.75	0.9802
C^2	1.44	0.9802
D^2	-3.19	0.9802

Table 4. Adequacy of the model tested for the process of chromium adsorption over CNP.

Source	Sequential p-value	Lack of Fit p-value	Adjusted R^2	Predicted R^2
Linear	< 0.0001	< 0.0001	0.6857	0.6102
2FI	0.9207	< 0.0001	0.6089	0.3612
Quadratic	< 0.0001	0.0004	0.9763	0.8859
Cubic	0.1299	0.0003	0.9866	-

Based on Table 5, the model's significance is demonstrated by its F-value of 74.65. Such a high F-value is only expected to occur by chance at a rate of 0.01 percent, suggesting that the model is reliable. The key model terms in this instance are those with a P-value lower than 0.0500, namely B, D, BD, A2, B2, and D2. Furthermore, the F-value for the lack of fit is 42.18, indicating its significance. A large F-value for the lack of fit, such as this, would typically only occur due to noise about 0.04 percent of the time. The anticipated R^2 value of 0.8859 falls within 0.2 of the Adjusted R^2 value of 0.9763, implying that the disparity is under 0.2. The ratio of signal to noise is determined by the precision's suitability, which was found to be 24.82, indicating an acceptable signal (preferably 4).

Table 5. ANNOVA and fit statistics.

Source	Sum of Squares	Mean Square	F-value	p-value
Model	13894.25	992.45	74.65	< 0.0001
A-Cr Conc	7.42	7.42	0.5581	0.4707
B-CNP Conc	10927.42	10927.42	821.89	< 0.0001
C-Time	24.38	24.38	1.83	0.2029
D-pH	424.38	424.38	31.92	0.0001
AB	12.25	12.25	0.9214	0.3577
AC	4.00	4.00	0.3009	0.5943
AD	36.00	36.00	2.71	0.1281
BC	64.00	64.00	4.81	0.0506
BD	289.00	289.00	21.74	0.0007
CD	6.25	6.25	0.4701	0.5071
A^2	399.78	399.78	30.07	0.0002
B^2	2249.51	2249.51	169.19	< 0.0001
C^2	28.59	28.59	2.15	0.1705
D^2	140.59	140.59	10.57	0.0077
Residual	146.25	13.30	-	-
Lack of Fit	143.42	23.90	42.18	0.0004
Pure Error	2.83	0.5667	-	-
Cor Total	14040.50	-	-	-

This model is valuable in navigating the design space. The coefficient estimate shows the expected variation in response per unit change in the factor value, all other things being equal. The intercept in an orthogonal design denotes the overall average response across all runs. The coefficients are modifications based on the setting of the factors surrounding that average.

Anupam et al. (2011) investigated how carbon nanoparticles can be used to remove HC by studying four parameters that impact removal efficiency. A close fit between the observed R^2 value of 0.9763 and the predicted R^2 value of 0.8859 was found for the proposed second order polynomial model. In addition, the ANOVA (analysis of variance) of the regression model showed high significance, as well as a very low P-value (0.000) and an F-value of 31.52. The predicted R^2 of 0.7409 and the adjusted R^2 of 0.9353 were largely in agreement. The ANOVA results indicated that the linear effects of pH (P = 0.000), nanoparticle concentration (P = 0.000), and time (P = 0.002) were significant, as were the square effects of nanoparticle concentration (P = 0.003) and time (P = 0.000). Moreover, the square effects of pH, nanoparticle concentration, and time (P = 0.000) were significant, while the interactive effects of pH with nanoparticle concentration (P = 0.397), pH with time (P = 0.154), and nanoparticle concentration with time (P = 0.718) had no effect on chromium extraction [66].

3.3. Final Equation in Terms of Coded Factors

A second-order polynomial equation (Eq. (4)) incorporating interaction terms was used to create a quadratic model based on the obtained experimental data using CCD. The resulting equation is shown below, expressed in terms of coded factors.

$$\text{Removal efficiency} = +74.17 - 0.6667A + 25.58B + 1.21C - 5.04D + 0.8750AB - 0.5000AC - 1.50AD + 2.00BC - 4.25BD + 0.6250CD - 5.37A^2 - 12.75B^2 + 1.44C^2 - 3.19D^2 \quad (4)$$

The equation was used in terms of coded factors in order to predict the response for different levels of every factor. The default coding for more levels of the factors was +1, whereas the coding for less levels was -1. The coded equation was used to calculate the factors' relative weights by examining their coefficients.

3.4. 2D and 3D Surface Analysis

3.4.1. Cr concentration vs CNP concentration

The CNP was found to have a maximum chromium removal efficiency of 83% when the initial Cr concentration was 100 ppm and the adsorbent

dose was 10 g per L. The time and pH remained constant at 30 min and 2, respectively. Figures 9(a) and (b) show that the removal efficiency increased and the initial concentration of chromium rose from 10 ppm to 100 ppm as the adsorbent dose was increased from 1 g/L to 10 g/L.

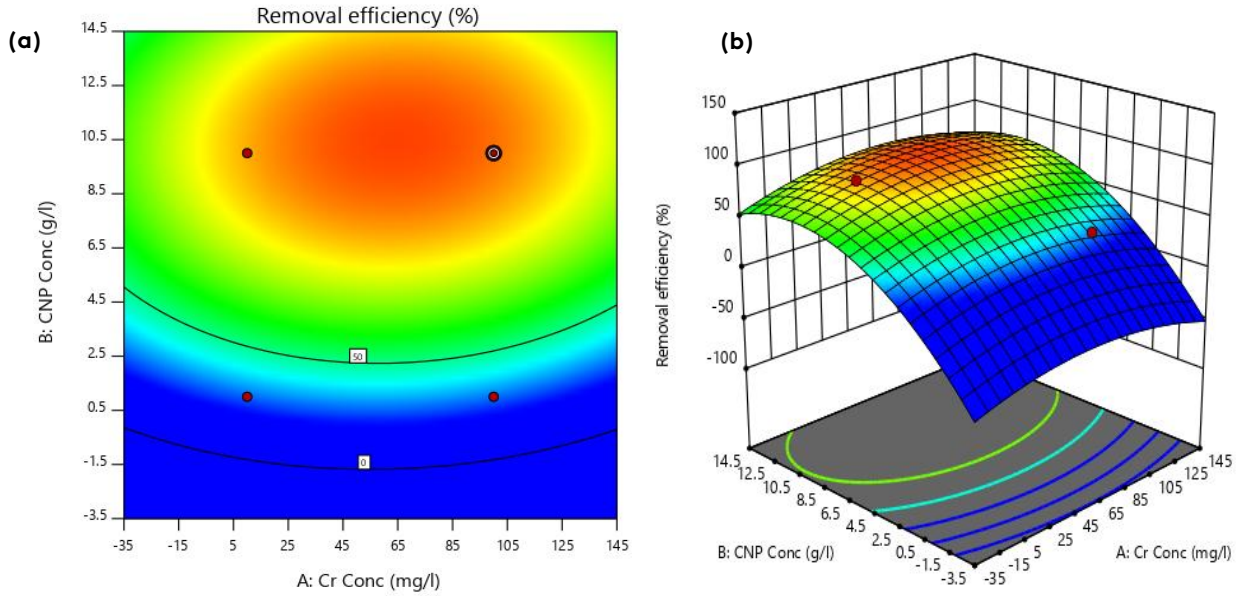

Fig. 9. Synergistic effect of CNP dosage and initial Cr concentration on removal efficiency: (a) 2D Contour Plot and (b) 3DSurface Plot [Constant parameters: Time = 30 min and pH = 2].

Based on the literature, it has been observed that the correlation between the initial concentration of HC and the dosage of the adsorbent is essential for the effective removal of chromium (VI). Additionally, we have determined that the dosage of the adsorbent and the initial concentration of HC in the feed, with regard to chromium (VI) adsorption, are influenced by temperature and pH. In a prior study, it was demonstrated that the highest level of chromium adsorption occurred at a pH of 2 and a temperature of 30 °C, resulting in the greatest removal effectiveness of 86% [67,68].

A study indicated that both the algal biomass and the chromium concentration initially present were important variables controlling the removal of arsenic by the algae. A higher algal biomass and lower chromium concentration provided better conditions for the removal of chromium from the solution, because the lighter weight of the sorbent provides less biosorption active sites and thus more competition occurs between protons and metal ions competing for the limited number of biosorption active sites [69].

3.4.2. Cr concentration vs Time

In accordance with this study, chromium was reduced by up to 83% when the initial chromium concentration was 100 mg/L, the contact time for the reduction was 30 min, and the solution was kept at a pH of 2 while the CNP concentration remained at 10 g/L. Based on the figures presented in 10(a) and 10(b), it is evident that increasing the CNP concentration from 1 g/L to 10 g/L resulted in a higher removal efficiency, while lowering the removal effectiveness from pH 2 to pH 9. Additionally, the surface plot provided insight investigation into the effects of heavy metal biosorption on initial concentrations of heavy metals and reaction time.

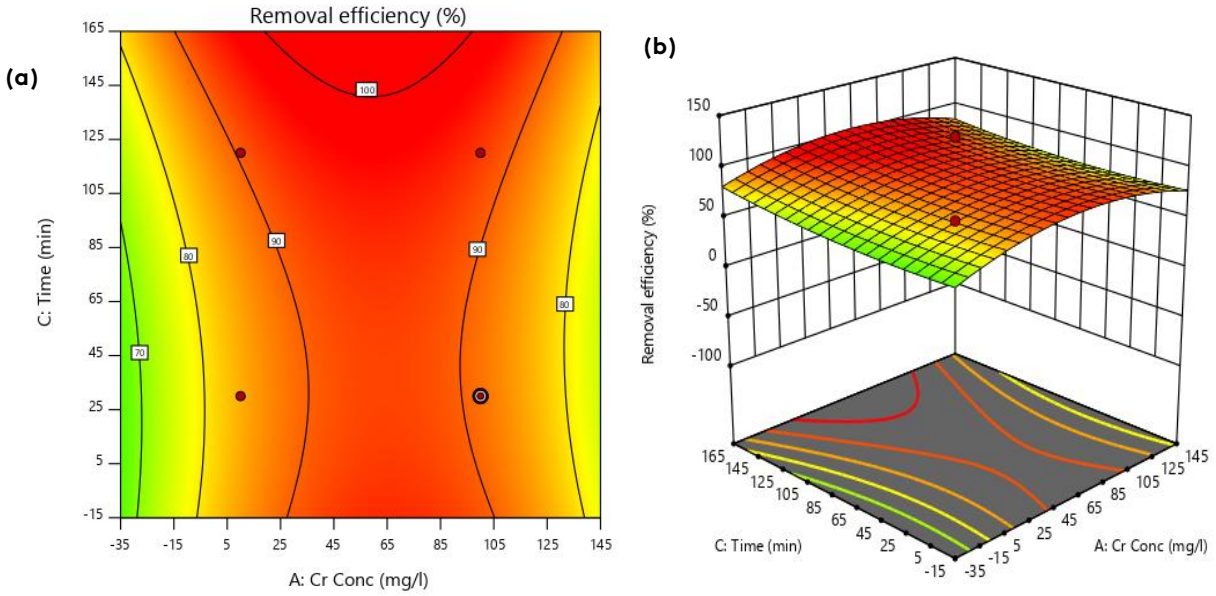

Fig. 10. Synergistic effect of contact time and initial Cr concentration on removal efficiency: (a) 2D Contour Plot and (b) 3DSurface Plot [Constant parameters: CNP dosage = 10 g/L and pH = 2].

According to Jaafari & Yaghmaeian (2019), the amount of chromium removed increased when the reaction time varied from 30 to 100 hours, but then diminished gradually. Another study reported that the initial concentration of heavy metal ions and the quantity of adsorbent used have a significant impact on the adsorption efficiency. The surface plots illustrate the effectiveness of heavy metal ion adsorption as a function of both initial ion concentration and removal time. Furthermore, in the case of Cu2+ and Ni2+, under conditions of constant removal time, the adsorption efficiency decreased as the concentration of heavy metal ions rose. However, for Pb2+, the removal effectiveness increased up to 500 ppm, and it decreased significantly. This is because there were not sufficient active sites on the adsorbent's surface to adsorb the toxic metal ions beyond a certain concentration [70].

3.4.3. Cr concentration vs pH

Figures 11(a) and (b) indicate that the initial Cr concentration and removal efficiency increase together. In contrast, as the pH rises, the removal efficiency falls. The research revealed that the greatest removal efficiency reached 83% when the CNP concentration and reaction time were held constant at 10 g/L and 30 min, respectively. The study was conducted at a pH of 2, with an initial chromium concentration of 10 mg/L.

Another research project conducted a study on the overall impact of pH and initial HC concentration on the adsorption of HC and presented the results as three-dimensional response surfaces. The study found that, at a temperature and constant adsorbent dose of 30 °C and 3 g/L, respectively, the maximum chromium adsorption rate was greater than 76% [68]. The surface plot indicates that there is a correlation between the pH and initial concentration, whereas when the initial concentration rises, the removal percentage falls but increases as the pH level increases [71].

3.4.4. CNP concentration vs Time

In Figures 12(a) and (b), it is demonstrated that the highest removal efficiency achieved was 83%.

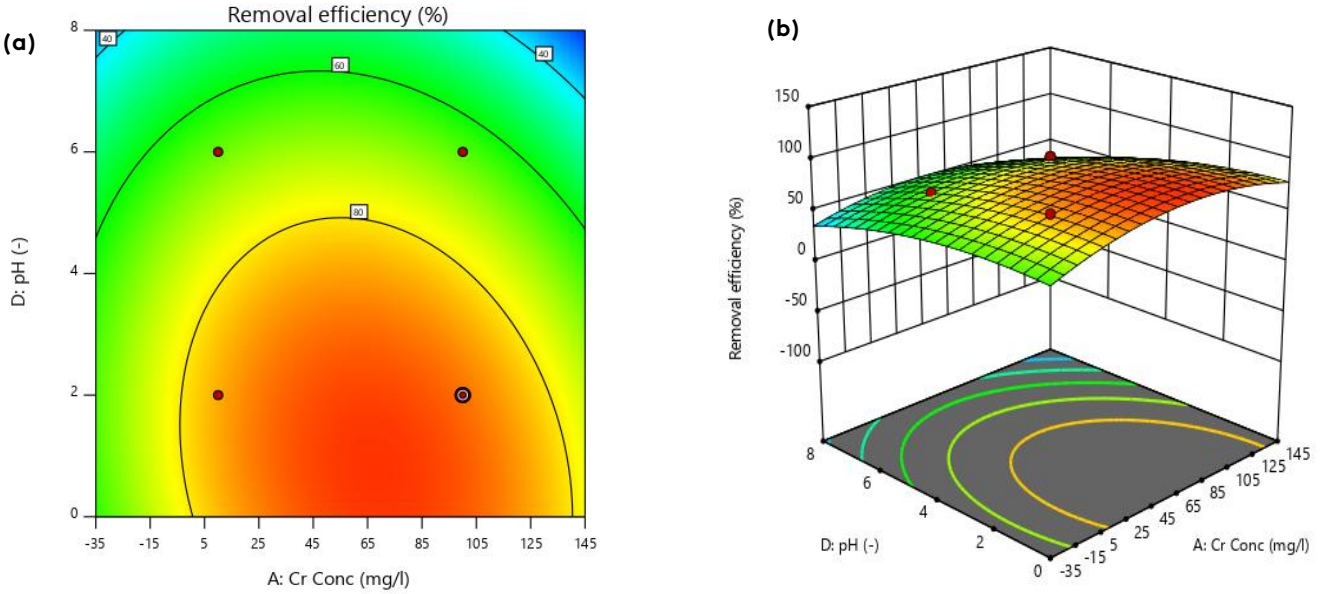

Fig. 11. Synergetic effect of pH and initial Cr concentration on removal efficiency: (a) 2D Contour Plot and (b) 3D Surface Plot [Constant parameters: Time = 30 min and CNP = 10 g/L]

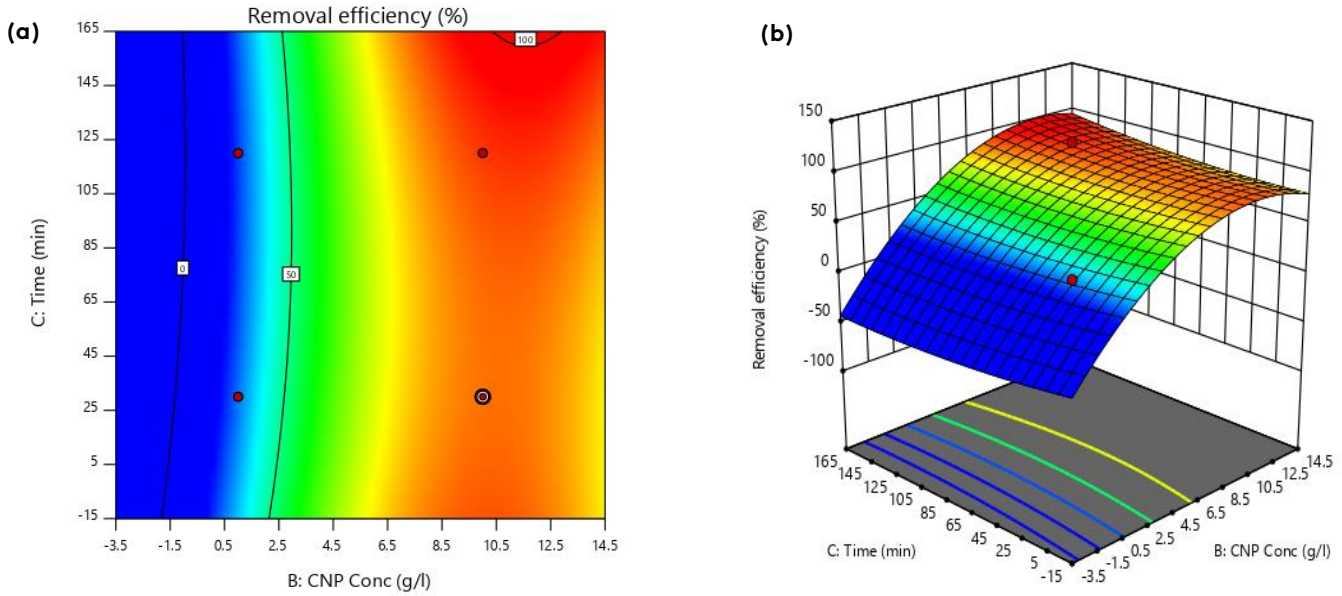

Fig. 12. Synergistic effect of contact time and CNP dosage on removal efficiency: (a) 2D Contour plot and (b) 3D Surface plot [Constant parameters: Cr = 100 ppm and pH = 2].

This occurred when the reaction time was set at 30 min and the CNP concentration was 10 g/L. The initial concentration of chromium was kept steady at 100 mg/L, and the pH was kept steady at 2.

The findings demonstrate that the removal effectiveness increased along with the CNP concentration and time.

A study stated that, as the time varied from 30 to 100 hours, heavy metal removal was found to increase linearly up to 96 percent with increased amounts of algae used. Metal biosorption using *C.coloniales* algae exhibited rapid uptake over the first 100 hours of exposure [69].

3.4.5. CNP concentration vs pH

From Figures 13(a) and (b), a correlation is shown to exists between CNP concentration and removal efficiency. The experiment was carried out under a constant time of 30 min and a pH of 2, a CNP concentration of 10 g/L and a starting concentration of chromium of 100 mg/L.

A research report indicated that when an activated carbon sample weighing one gram was used to treat a pH 4.0 solution that is made up of water, it was found that approximately 80% of HC was effectively adsorbed [67].

The surface plots showed that pH and adsorbent dosage are the most important variables for HC adsorption. When the adsorbent dosage increased, the rate of HC removal increased rapidly. Following the increase in the removal percentage of HC, it remained stable at an optimum point between 0.25-0.30g.

As adsorbent dose increases, there will be an increase in the number of adsorbent particles and therefore an increase in the available surface area of the adsorbents to adsorb more HC molecules [68].

A similar kind of study examined the influence of pH and the quantity of adsorbent on Cu (II) adsorption at an adsorption concentration of 30 mg/dm³.

The data collected from this research indicated that pH played an extremely significant role in the adsorption process; the greatest adsorption was observed at a pH of 5.5.

As such, the best pH levels to adsorb Ni (II) and Zn (II) ions were determined to be 7.3 and 6.5, respectively, because the surface charge of the adsorbent was influenced by pH. In addition, increasing the quantity of the adsorbent led to a rapid increase in the extent of adsorption, due to an increase in the adsorbent surface area [72].

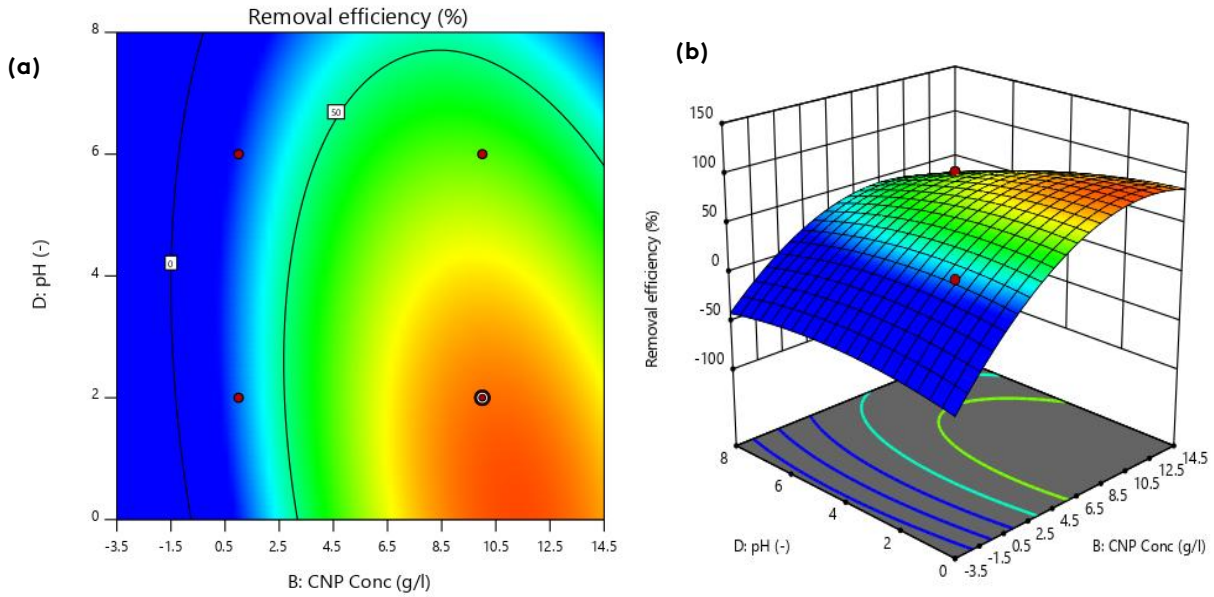

Fig. 13. Synergistic effect of pH and CNP dosage on removal efficiency: (a) 2D Contour Plot and (b) 3D Surface Plot [Constant parameters: Cr = 100 ppm and Time = 30 min].

3.4.6. Time vs pH

The results of an experiment conducted for 30 min at a pH level of 2 reveal that 83% was the greatest rate of elimination, with an initial concentration of 100 mg per L of Cr and a CNP concentration of 10 g per L that remained constant throughout the experiment.

The data presented in Figures 14(a) and (b) indicate that the removal efficiency improved as the contact time between the substances increased, but it declined as the pH level increased. It was reported in a study that the 3D plot of pH and contact time showed 66 percent adsorption at a pH of 7 within 30 min. Following that, the Fe_3O_4 nanoparticles achieved maximum adsorption (98 percent) at 40 °C and pH 6 in another 10 min [73].

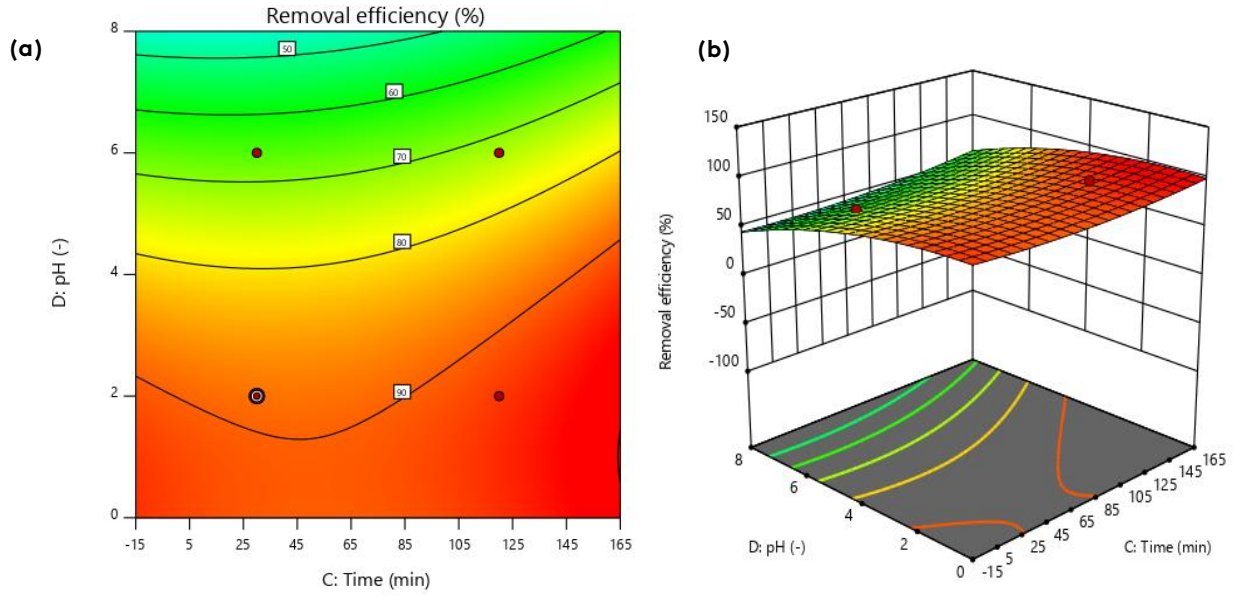

Fig. 14. Synergistic effect of pH and contact time on removal efficiency: (a) 2D Contour plot and (b) 3D surface plot [Constant parameters: Cr = 100 ppm and CNP = 10 g/L].

4. Conclusion

The potential of carbon nanoparticles derived from leaves of the *Cocos nucifera* for the removal of chromium contamination in leather industry effluents has not been previously explored. Encouraging results were obtained under optimized conditions in the batch adsorption experiments conducted for this study, indicating the possibility of extending these experiments to a continuous mode with a greater capacity in the near future. Modifying the CNPs by producing nanocomposites to enhance their adsorption ability can be most effective in the bioremediation of heavy metal pollution. The combination of rigorous process optimization (RSM), comprehensive material characterization, and detailed mechanistic investigation through isotherm modeling has provided a holistic understanding of this biosorption system. The findings strongly support the potential for transitioning this technology from laboratory to industrial scale for the treatment of chromium-contaminated wastewater in tanneries and other metal-finishing industries.

Acknowledgement

The corresponding author would like to sincerely thank the principal and the management for providing a seed money grant (Reference: VH/R&D/SMP/22-23/006) to support and encourage research activities.

Author's contribution

S.R.A.: Conceptualization, methodology, supervision, project administration, funding acquisition, and writing review and editing. A.K.S.: Investigation, experimentation, data collection, formal analysis, and writing original draft. V.M.P.: Investigation, data curation and validation. B.B.: Methodology, validation and interpretation of results. V.J.: Formal analysis, visualization and validation. S.K.G.: Software, computational analysis and data visualization. M.S.A.: Methodology & interpretation of results.. All authors have read and approved the final version of the manuscript.

Conflict of interest

No potential conflict of interest was reported by the authors.

Data availability

The datasets generated and/or analyzed during the current study are available with the corresponding author and shall be provided on reasonable request.

Funding

This research was supported by the Seed Money Grant provided by the management of Vel Tech High Tech Dr. Rangarajan Dr. Sakunthala Engineering College, Chennai, India, under Grant Reference No. VH/R&D/SMP/22-23/006.

Declaration of Using Generative AI

During the preparation of this manuscript, the authors used a generative artificial intelligence tool solely for language improvement, grammatical correction, and enhancement of the clarity of the text. The authors carefully reviewed and edited all AI-assisted content and take full responsibility for the accuracy, originality, integrity, and final content of the manuscript. Generative AI was not used to generate experimental data, analyze results, create scientific conclusions, or replace the authors' intellectual contributions

References

[1] Bo, J., & Muyiwa, A. (n.d.). Effects of alkaloids of Cocos nucifera husk fibre on cardiovascular disease indices in albino mice. *Cardiovascular Pharmacology: Open Access*, 1–6. https://doi.org/10.35248/2329-6607.19.8.253

[2] Adkins, S. W., Biddle, J., Nguyen, Q. T., & Foale, M. (2020). Cocos nucifera coconut. In *Biotechnology of fruit and nut crops* (pp. 79–91). https://doi.org/10.1079/9781780648279.0079

[3] Clarissa, J. T. (2014). *Cocobestie: Hair benefits from Cocos nucifera oil*.

[4] Krishnaveni Dhanuskodi, K. P. S. A., & P. S. (2023). Chromium-sorbed maize stalk biochar and its power benefited disposal: An effective power generation method for removal of chromium. *Water, Air, & Soil Pollution, 234*(222). https://doi.org/10.1007/s11270-023-06233-8

[5] Momen, A. H. A., Nur, M. H. S., & Sheikh, A. T. H. R. (2018). Chromium removal from tannery wastewater using Syzygium cumini bark adsorbent. *International Journal of Environmental Science and Technology*. https://doi.org/10.1007/s13762-018-1714-y

[6] Roy, C. (2012). A study on environmental compliance of Indian leather industry & its far-reaching impact on leather exports. *Foreign Trade Review, 47*(2), 3–36. https://doi.org/10.1177/0015732515120201

[7] Mandal, T., Dasgupta, D., Mandal, S., & Datta, S. (2010). Treatment of leather industry wastewater by aerobic biological and Fenton oxidation process. *Journal of Hazardous Materials, 180*(1–3), 204–211. https://doi.org/10.1016/j.jhazmat.2010.04.014

[8] Urfi Jahan, U. K., Mohd Irfan Naikoo, M. K., M. H., & F. A. K. (2023). Trophic transfer, bioaccumulation, and detoxification of lead and zinc via sewage sludge applied soil-barley-aphid-ladybird food chain. *Water, Air, & Soil Pollution, 234*(508). https://doi.org/10.1007/s11270-023-06531-1

[9] Tunç, İ. G., & M. (2022). Palladium nanoparticles supported on activated carbon (C) for the catalytic hexavalent chromium reduction. *Water, Air, & Soil Pollution, 233*(4). https://doi.org/10.1007/s11270-021-05479-4

[10] Singanan, M., & Peters, E. (2013). Removal of toxic heavy metals from synthetic wastewater using a novel biocarbon technology. *Journal of Environmental Chemical Engineering, 1*(4), 884–890. https://doi.org/10.1016/j.jece.2013.07.030

[11] Patil, N. I., & Y. (2022). Assessing physicochemical technologies for removing hexavalent chromium from contaminated waters—An overview and future research directions. *Water, Air, & Soil Pollution, 233*(355). https://doi.org/10.1007/s11270-022-05745-z

[12] Zoufri, I., Merzouki, M., Ammari, M., El-Byari, Y., & Bari, A. (2024). Investigation of the physicochemical and microbiological quality of brassware effluents: Insight into the charge of heavy metal and pollutants in wastewater from Fez, Morocco. *Advances in Environmental Technology, 10*(1), 41–54. https://doi.org/10.22104/aet.2024.6382.1748

[13] Sailo, R. R. L. (2017). Efficient chromium recovery from tannery sludge for sustainable management. *International Journal of Environmental Science and Technology*. https://doi.org/10.1007/s13762-017-1244-z

[14] Akanksha Gupta, A. S., & V. K. M. (2023). Hexavalent Cr, its toxicity and removal strategy: Revealing PGPB potential in its remediation. *Water, Air, & Soil Pollution, 234*(492). https://doi.org/10.1007/s11270-023-06477-4

[15] Briffa, J., Sinagra, E., & Blundell, R. (2020). Heavy metal pollution in the environment and their toxicological effects on humans. *Heliyon, 6*(9), Article e04691.

https://doi.org/10.1016/j.heliyon.2020.e04691

[16] Cheraghi, M., Zahiri, J., Moradi Sabzkouhi, A., & Moradi, S. (2024). Evaluation of the heavy metal risk potential in salts extracted from the Shorbarik River. *Advances in Environmental Technology, 10*(2), 160–169. https://doi.org/10.22104/aet.2024.6707.1831

[17] Sun, H., Brocato, J., & Costa, M. (2015). Oral chromium exposure and toxicity. *Current Environmental Health Reports, 2*(3), 295–303. https://doi.org/10.1007/s40572-015-0054-z

[18] Nur-E-Alam, M., Mia, M. A. S., Ahmad, F., & Rahman, M. M. (2020). An overview of chromium removal techniques from tannery effluent. *Applied Water Science, 10*(9). https://doi.org/10.1007/s13201-020-01286-0

[19] Razmgar, K., & Hosseini, Z. B. M. (2016). Removal of As(V), Cr(VI) and Pb(II) from aqueous solution using surfactant-modified Sabzevar nanozeolite. *Advances in Environmental Technology, 2*(2), 105–109. https://doi.org/10.22104/AET.2016.398

[20] Rajasulochana, P., & Preethy, V. (2016). Comparison on efficiency of various techniques in treatment of waste and sewage water – A comprehensive review. *Resource-Efficient Technologies, 2*(4), 175–184. https://doi.org/10.1016/j.reffit.2016.09.004

[21] V, Y., & AK, P. (2016). Removal of hexavalent chromium (Cr6+) using different natural adsorbents - A review. *Journal of Chromatography & Separation Techniques, 8*(06), 6–11. https://doi.org/10.4172/2157-7064.1000392

[22] Lianpeng Yan, K. Z. R., & X. Z. (2023). Efficient adsorption of anionic azo dye in wastewater with medulla tetrapanacis modified by cationic surfactant. *Water, Air, & Soil Pollution, 234*(511). https://doi.org/10.1007/s11270-023-06464-9

[23] Fotini Noli, A. D., Catherine Dendrinou-Samara, M. K., & E. P. (2022). Critical parameters and mechanisms of chromium removal from water by copper-based nanoparticles. *Water, Air, & Soil Pollution, 234*(12). https://doi.org/10.1007/s11270-022-06009-6

[24] Sekar, S., Mahadevan, S., Deepa, P. R., Shanmugam, B. K., Kumar, B. V. N. P., & Mandal, A. B. (2013). The metabolic advantage of choline lactate in growth media: An experimental analysis with staphylococcus lentus. *Applied Biochemistry and Biotechnology, 169*(2), 380–392. https://doi.org/10.1007/s12010-012-9981-4

[25] Gupta, V. K., Agarwal, S., & Saleh, T. A. (2011). Synthesis and characterization of alumina-coated carbon nanotubes and their application for lead removal. *Journal of Hazardous Materials, 185*(1), 17–23. https://doi.org/10.1016/j.jhazmat.2010.08.053

[26] Kumar, A., & Jena, H. M. (2017). Adsorption of Cr(VI) from aqueous phase by high surface area activated carbon prepared by chemical activation with ZnCl2. *Process Safety and Environmental Protection, 109*, 63–71. https://doi.org/10.1016/j.psep.2017.03.032

[27] Almohammadi, S., & Mirzaei, M. (2016). Removal of copper (II) from aqueous solutions by adsorption onto granular activated carbon in the presence of competitor ions. *Advances in Environmental Technology, 2*(2), 85–94. https://doi.org/10.22104/AET.2016.392

[28] Mohan, G. V. K., Babu, A. N., & Ravindhranath, K. K. (2017). Removal of chromium (VI) from water using adsorbent derived from spent coffee grounds. *International Journal of Environmental Science and Technology*. https://doi.org/10.1007/s13762-017-1593-7

[29] Behnajady, S. G. M. A. (2016). Chromium (VI) adsorption from aqueous solution by prepared biochar from Onopordom heteracanthom. *International Journal of Environmental Science and Technology*. https://doi.org/10.1007/s13762-016-0978-3

[30] Rao, G. G. A. H. V. M. (2014). Removal of hexavalent chromium from aqueous solutions using barks of Acacia albida and leaves of Euclea schimperi. *International Journal of Environmental Science and Technology*. https://doi.org/10.1007/s13762-014-0530-2

[31] Ghaneian, M. T., Bhatnagar, A., Ehrampoush, M. H., Amrollahi, M., Jamshidi, B., Dehvari, M., & Taghavi, M. (2017). Biosorption of hexavalent chromium from aqueous solution onto pomegranate seeds: Kinetic modeling studies. *International Journal of Environmental Science and Technology*. https://doi.org/10.1007/s13762-016-1216-8

[32] Bajpai, S., Dey, A., Jha, M. K., Gupta, S. K., & Gupta, A. (2012). Removal of hazardous hexavalent chromium from aqueous solution using divinylbenzene copolymer resin. *International Journal of Environmental Science and Technology*, 683–690. https://doi.org/10.1007/s13762-012-0099-6

[33] Lataye, K. M. D., & Kurwadkar, V. M. S. (2016). Adsorption of hexavalent chromium onto activated carbon derived from Leucaena leucocephala waste sawdust: Kinetics, equilibrium and thermodynamics. *International Journal of Environmental Science and Technology, 13*(9), 2107–2116. https://doi.org/10.1007/s13762-016-1042-z

[34] Chandana, L., Krushnamurty, K., Suryakala, D., & Subrahmanyam, C. (2018). Low-cost adsorbent derived from the coconut shell for the removal of hexavalent chromium from aqueous medium. *Materials Today: Proceedings, 26*, 44–51. https://doi.org/10.1016/j.matpr.2019.04.205

[35] Abshirini, Y., Foroutan, R., & Esmaeili, H. (2019). Cr(VI) removal from aqueous solution using activated carbon prepared from Ziziphus spina-christi leaf. *Materials Research Express, 6*(4). https://doi.org/10.1088/2053-1591/aafb45

[36] Yusuff, A. S. (2019). Adsorption of hexavalent chromium from aqueous solution by Leucaena leucocephala seed pod activated carbon: Equilibrium, kinetic and thermodynamic studies. *Arab Journal of Basic and Applied Sciences, 26*(1), 1–14. https://doi.org/10.1080/25765299.2019.1567656

[37] Sahlabji, T., El-Nemr, M. A., El Nemr, A., Ragab, S., Alghamdi, M. M., El-Zahhar, A. A., Idris, A. M., & Said, T. O. (2022). High surface area microporous activated carbon from Pisum sativum peels for hexavalent chromium removal from aquatic environment. *Toxin Reviews, 41*(2), 639–649. https://doi.org/10.1080/15569543.2021.1908361

[38] Ma, H., Yang, J., Gao, X., Liu, Z., Liu, X., & Xu, Z. (2019). Removal of chromium (VI) from water by porous carbon derived from corn straw: Influencing factors, regeneration and mechanism. *Journal of Hazardous Materials, 369*, 550–560. https://doi.org/10.1016/j.jhazmat.2019.02.063

[39] Ali, I. H., Mesfer, M. K. Al, Khan, M. I., & Danish, M. (2019). Exploring adsorption process of lead (II) and chromium (VI) ions from aqueous solutions on acid activated carbon prepared from… *Processes, 7*(2), 217.

[40] Obayomi, K. S., Bello, J. O., Yahya, M. D., Chukwunedum, E., & Adeoye, J. B. (2020). Statistical analyses on effective removal of cadmium and hexavalent chromium ions by multiwall carbon nanotubes (MWCNTs). *Heliyon, 6*(6), Article e04174. https://doi.org/10.1016/j.heliyon.2020.e04174

[41] Nowruzi, R., Heydari, M., & Javanbakht, V. (2020). Synthesis of a chitosan/polyvinyl alcohol/activate carbon biocomposite for removal of hexavalent chromium from aqueous solution. *International Journal of Biological Macromolecules, 147*, 209–216. https://doi.org/10.1016/j.ijbiomac.2020.01.044

[42] Tu, B., Wen, R., Wang, K., Cheng, Y., Deng, Y., Cao, W., Zhang, K., & Tao, H. (2020). Efficient removal of aqueous hexavalent chromium by activated carbon derived from Bermuda grass. *Journal of Colloid and Interface Science, 560*, 649–658. https://doi.org/10.1016/j.jcis.2019.10.103

[43] Ravulapalli, S., & Ravindhranath, K. (2018). Enhanced removal of chromium (VI) from wastewater using active carbon derived from Lantana camara plant as adsorbent. *Water Science and Technology, 78*(6), 1377–1389. https://doi.org/10.2166/wst.2018.413

[44] Norouzi, S., Heidari, M., Alipour, V., Rahmanian, O., Fazlzadeh, M., Mohammadi-moghadam, F., Nourmoradi, H., Goudarzi, B., & Dindarloo, K. (2018). Preparation, characterization and Cr(VI) adsorption evaluation of NaOH-activated carbon produced from Date Press Cake; an agro-industrial waste. *Bioresource Technology, 258*, 48–56. https://doi.org/10.1016/j.biortech.2018.02.106

[45] Niazi, L., Lashanizadegan, A., & Sharififard, H. (2018). Chestnut oak shells activated carbon: Preparation, characterization and application for Cr (VI) removal from dilute aqueous solutions. *Journal of Cleaner Production, 185*, 554–561. https://doi.org/10.1016/j.jclepro.2018.03.026

[46] Guo, H., Bi, C., Zeng, C., Ma, W., Yan, L., Li, K., & Wei, K. (2018). Camellia oleifera seed shell carbon as an efficient renewable bio-adsorbent for the adsorption removal of hexavalent chromium and methylene blue from aqueous solution. *Journal of Molecular Liquids, 249*, 629–636. https://doi.org/10.1016/j.molliq.2017.11.096

[47] Rai, M. K., Giri, B. S., Nath, Y., Bajaj, H., Soni, S., Singh, R. P., Singh, R. S., & Rai, B. N. (2018). Adsorption of hexavalent chromium from aqueous solution by activated carbon prepared from almond shell: Kinetics, equilibrium and thermodynamics study. *Journal of Water Supply: Research and Technology - AQUA, 67*(8), 724–737. https://doi.org/10.2166/aqua.2018.047

[48] Labied, R., Benturki, O., Eddine Hamitouche, A. Y., & Donnot, A. (2018). Adsorption of hexavalent

chromium by activated carbon obtained from a waste lignocellulosic material (Ziziphus jujuba cores): Kinetic, equilibrium, and thermodynamic study. *Adsorption Science and Technology, 36*(3–4), 1066–1099. https://doi.org/10.1177/0263617417750739

[49] Berihun, D. (2017). Removal of chromium from industrial wastewater by adsorption using coffee husk. *Journal of Material Science & Engineering, 6*(02), 6–11. https://doi.org/10.4172/2169-0022.1000331

[50] Rai, M. K., Shahi, G., Meena, V., Meena, R., Chakraborty, S., Singh, R. S., & Rai, B. N. (2016). Removal of hexavalent chromium Cr (VI) using activated carbon prepared from mango kernel activated with H3PO4. *Resource-Efficient Technologies, 2*, S63–S70. https://doi.org/10.1016/j.reffit.2016.11.011

[51] Gueye, M., Richardson, Y., Kafack, F. T., & Blin, J. (2014). High efficiency activated carbons from African biomass residues for the removal of chromium(VI) from wastewater. *Journal of Environmental Chemical Engineering, 2*(1), 273–281. https://doi.org/10.1016/j.jece.2013.12.014

[52] Parthasarathy, P., & Narayanan, S. K. (2014). Effect of hydrothermal carbonization reaction parameters on… *Environmental Progress & Sustainable Energy, 33*(3), 676–680. https://doi.org/10.1002/ep

[53] Yi, Z. C., Luo, S. M., Li, G., Li, H. S., & Lin, H. M. (2013). Removal of Cr(VI) from aqueous solution using activated carbon prepared from several agriculture by-products. *Advanced Materials Research, 807–809*, 582–590. https://doi.org/10.4028/www.scientific.net/AMR.807-809.582

[54] Thamilarasu, P., & Karunakaran, K. (2013). Kinetic, equilibrium and thermodynamic studies on removal of Cr(VI) by activated carbon prepared from Ricinus communis seed shell. *Canadian Journal of Chemical Engineering, 91*(1), 9–18. https://doi.org/10.1002/cjce.20675

[55] Acharya, J., Sahu, J. N., Sahoo, B. K., Mohanty, C. R., & Meikap, B. C. (2009). Removal of chromium(VI) from wastewater by activated carbon developed from Tamarind wood activated with zinc chloride. *Chemical Engineering Journal, 150*(1), 25–39. https://doi.org/10.1016/j.cej.2008.11.035

[56] El Nemr, A. (2009). Potential of pomegranate husk carbon for Cr(VI) removal from wastewater: Kinetic and isotherm studies. *Journal of Hazardous Materials, 161*(1), 132–141. https://doi.org/10.1016/j.jhazmat.2008.03.093

[57] El Nemr, A., Khaled, A., Abdelwahab, O., & El-Sikaily, A. (2008). Treatment of wastewater containing toxic chromium using new activated carbon developed from date palm seed. *Journal of Hazardous Materials, 152*(1), 263–275. https://doi.org/10.1016/j.jhazmat.2007.06.091

[58] El-Sikaily, A., El Nemr, A., Khaled, A., & Abdelwehab, O. (2007). Removal of toxic chromium from wastewater using green alga Ulva lactuca and its activated carbon. *Journal of Hazardous Materials, 148*(1–2), 216–228. https://doi.org/10.1016/j.jhazmat.2007.01.146

[59] Gottipati, R., & Mishra, S. (2016). Preparation of microporous activated carbon from Aegle marmelos fruit shell and its application in removal of chromium(VI) from aqueous phase. *Journal of Industrial and Engineering Chemistry, 36*, 355–363. https://doi.org/10.1016/j.jiec.2016.03.005

[60] Yang, J., Yu, M., & Chen, W. (2015). Adsorption of hexavalent chromium from aqueous solution by activated carbon prepared from longan seed: Kinetics, equilibrium and thermodynamics. *Journal of Industrial and Engineering Chemistry, 21*, 414–422. https://doi.org/10.1016/j.jiec.2014.02.054

[61] Goswami, M., Borah, L., Mahanta, D., & Phukan, P. (2014). Equilibrium modeling, kinetic and thermodynamic studies on the adsorption of Cr(VI) using activated carbon derived from matured tea leaves. *Journal of Porous Materials, 21*(6), 1025–1034. https://doi.org/10.1007/s10934-014-9852-1

[62] Gupta, S., & Babu, B. V. (2009). Utilization of waste product (tamarind seeds) for the removal of Cr(VI) from aqueous solutions: Equilibrium, kinetics, and regeneration studies. *Journal of Environmental Management, 90*(10), 3013–3022. https://doi.org/10.1016/j.jenvman.2009.04.006

[63] Hsu, N. H., Wang, S. L., Liao, Y. H., Huang, S. T., Tzou, Y. M., & Huang, Y. M. (2009). Removal of hexavalent chromium from acidic aqueous solutions using rice straw-derived carbon. *Journal of Hazardous Materials, 171*(1–3), 1066–1070. https://doi.org/10.1016/j.jhazmat.2009.06.112

[64] Mohanty, K., Jha, M., Meikap, B. C., & Biswas, M. N. (2005). Removal of chromium (VI) from dilute

aqueous solutions by activated carbon developed from Terminalia arjuna nuts activated with zinc chloride. *Chemical Engineering Science, 60*(11), 3049–3059. https://doi.org/10.1016/j.ces.2004.12.049

[65] Karthikeyan, T., Rajgopal, S., & Miranda, L. R. (2005). Chromium(VI) adsorption from aqueous solution by Hevea brasiliensis sawdust activated carbon. *Journal of Hazardous Materials, 124*(1–3), 192–199. https://doi.org/10.1016/j.jhazmat.2005.05.003

[66] Anupam, K., Dutta, S., Bhattacharjee, C., & Datta, S. (2011). Adsorptive removal of chromium (VI) from aqueous solution over powdered activated carbon: Optimisation through response surface methodology. *Chemical Engineering Journal, 173*(1), 135–143. https://doi.org/10.1016/j.cej.2011.07.049

[67] Yusuff, A. S. (2018). Optimization of adsorption of Cr(VI) from aqueous solution by Leucaena leucocephala seed shell activated carbon using design of experiment. *Applied Water Science, 8*(8), 1–11. https://doi.org/10.1007/s13201-018-0850-3

[68] Sahu, J. N., Acharya, J., & Meikap, B. C. (2009). Response surface modeling and optimization of chromium(VI) removal from aqueous solution using Tamarind wood activated carbon in batch process. *Journal of Hazardous Materials, 172*(2–3), 818–825. https://doi.org/10.1016/j.jhazmat.2009.07.075

[69] Jaafari, J., & Yaghmaeian, K. (2019). Optimization of heavy metal biosorption onto freshwater algae (Chlorella coloniales) using response surface methodology (RSM). *Chemosphere, 217*, 447–455. https://doi.org/10.1016/j.chemosphere.2018.10.205

[70] Kalantari, K., Ahmad, M. B., Fard Masoumi, H. R., Shameli, K., Basri, M., & Khandanlou, R. (2015). Rapid and high capacity adsorption of heavy metals by Fe3O4/montmorillonite nanocomposite using response surface methodology: Preparation, characterization, optimization, equilibrium isotherms, and adsorption kinetics study. *Journal of the Taiwan Institute of Chemical Engineers, 49*, 192–198. https://doi.org/10.1016/j.jtice.2014.10.025

[71] Afolabi, F. O., Musonge, P., & Bakare, B. F. (2021). Application of the response surface methodology in the removal of Cu2+ and Pb2+ from aqueous solutions using orange peels. *Scientific African, 13*, Article e00931. https://doi.org/10.1016/j.sciaf.2021.e00931

[72] Sarkar, M., & Majumdar, P. (2011). Application of response surface methodology for optimization of heavy metal biosorption using surfactant modified chitosan bead. *Chemical Engineering Journal, 175*(1), 376–387. https://doi.org/10.1016/j.cej.2011.09.125

[73] Singh, R., & Bhateria, R. (2020). Optimization and experimental design of the Pb2+ adsorption process on a nano-Fe3O4-based adsorbent using the response surface methodology. *ACS Omega, 5*(43), 28305–28318. https://doi.org/10.1021/acsomega.0c04284

How to cite this paper:

Saravana Raj, A., Karuppaiah Subramanian, A., Perumal,V. M., Balasubramanian, B., Jayabalan, V., Ganesan, S. K. & Akilan, M. S. (2026). Optimization studies of chromium biosorption by carbon nanoparticles of Cocos nucifera. *Advances in Environmental Technology*, 12(3), 375-395. DOI: 10.22104/aet.2026.7599.2132